water

MDPI

Article

Stable Isotope Composition of River Waters across the World

Yi Nan [1], Fuqiang Tian [1,*], Hongchang Hu [1], Lixin Wang [2] and Sihan Zhao [1]

[1] Department of Hydraulic Engineering, State Key Laboratory of Hydroscience and Engineering, Tsinghua University, Beijing 100084, China

[2] Department of Earth Sciences, Indiana University-Purdue University Indianapolis (IUPUI), Indianapolis, IN 46202, USA

* Correspondence: tianfq@tsinghua.edu.cn; Tel.: +86-10-6277-3396

Received: 1 July 2019; Accepted: 20 August 2019; Published: 23 August 2019

Abstract: Stable isotopes of O and H in water are meaningful indicators of hydrological and ecological patterns and processes. The Global Network of Isotopes in Precipitation (GNIP) and the Global Network of Isotopes in Rivers (GNIR) are the two most important global databases of isotopes in precipitation and rivers. While the data of GNIP is almost globally distributed, GNIR has an incomplete spatial coverage, which hinders the utilization of river isotopes to study global hydrological cycle. To fill this knowledge gap, this study supplements GNIR and provides a river isotope database with global-coverage by the meta-analysis method, i.e., collecting 17015 additional data points from 215 published articles. Based on the newly compiled database, we find that (1) the relationship between $\delta^{18}O$ and $\delta^{2}H$ in river waters exhibits an asymmetric imbricate feature, and bifurcation can be observed in Africa and North America, indicating the effect of evaporation on isotopes; (2) multiple regression analysis with geographical factors indicates that spatial patterns of river isotopes are quite different across regions; (3) multiple regression with geographical and meteorological factors can well predict the river isotopes, which provides regional regression models with r^2 of 0.50 to 0.89, and the best predictors in different regions are different. This work presents a global map of river isotopes and establishes a benchmark for further research on isotopes in rivers.

Keywords: isotopes; river isotopes; GNIR; meta-analysis

1. Introduction

Stable isotopes in water ($\delta^{2}H$ and $\delta^{18}O$) have been regarded as a powerful tool for investigating water source, flow paths and transit times [1] and solving large-scale water cycle problems [2]. Isotopic composition of water is affected by several environmental factors [3,4] and changes with multiple ecological and hydrological processes [5–7]. With growing interest in stable isotopes in water, many phenomena have been discovered which are usually difficult if not impossible to discern with conventional methods. For example, isotope data in rain, snow and streamflow from 254 watersheds indicated that a substantial proportion of global streamflow is younger than three months [8]. Based on the isotopes in 83 large lakes around the world, it was found that the terrestrial water fluxes are dominated by transpiration [9]. Also, isotopic data in plant xylem water, soil water, stream water, groundwater and precipitation water from 47 globally distributed sites were used to demonstrate that eco-hydrological separation is widespread across different biomes [10], which has been highlighted in many recent experimental or model studies (e.g., the work of measuring and modeling stable isotopes in mobile and bulk soil water conducted by Sprenger et al. [11]). providing a support for the "two water worlds" hypothesis [12]. These studies provide essentially new insights and evoke new questions for hydrological process understanding.

The spatial patterns of stable isotopes in different types of waters are fundamental for many isotopic studies and have been investigated by many researchers. Kendall and Coplen compiled a detailed map of stable isotopes in river water in the USA, and proposed river samples as proxies for average rain and recharge compositions [13]. Liu et al. (2014) presented the spatial pattern and seasonal variations in precipitation isotopes, and analyzed the correlations between isotopes and environmental variables based on the Chinese Network of Isotopes in Precipitation (CHNIP) dataset [14]. Zhao et al. (2017) provided the report of tap water isotopic composition over China based on a nation-wide volunteer network [15]. Such studies about water isotopes over large spatial scales not only help reveal the regional climatic and hydrologic features, but also provide a fundamental framework for local case studies [16].

The Global Network of Isotopes in Precipitation (GNIP) and the Global Network of Isotopes in Rivers (GNIR), which are the largest databases for monitoring isotopic compositions in precipitation and rivers, were launched in 1961 and 2007, respectively [17]. The Stable Water Vapor Isotope Database (SWVID) has been also developed recently for archiving high-frequency vapor isotope data collected with instruments based on infrared isotopic spectroscopy [18]. These databases present a relatively comprehensive pattern of isotopic compositions, and the large volume of data is helpful for achieving concrete conclusions. For example, GNIP and GNIR are the main data sources of the above mentioned research streamflow age conducted by Jasechko et al. [8].

However, while the data of GNIP is almost globally distributed, GNIR has a quite incomplete spatial coverage, with no or little data in many regions (Figure 1). As shown in Figure 1b, GNIR data are mainly distributed across the USA, Central Europe, South Central Asia, as well as several major rivers such as the Yangtze River in China, the Amazon River mainly located in Brazil and the Murray River in Australia. The incomplete spatial coverage of GNIR eventually also leads to a mismatch with GNIP in terms of data range, with only a few stream water $\delta^{18}O$ values lower than −20‰ in GNIR in comparison to GNIP with plenty of $\delta^{18}O$ values in the range of −40‰ to −20‰ [17,19]. This causes a spatial limitation on some global isotopic studies, e.g., the estimation of river age conducted by Jasechko et al. [8] only comprises roughly 20% of the globe's ice-free land area. Besides, it is found that globally fitted isoscapes of precipitation may have low accuracy and relevance when downscaled to regional levels [20]. This problem can be more serious for river water due to the data sparseness. Therefore, GNIR has obvious limitations in spatial coverage despite the fact that it is the most wide-spread available database of river water isotopes. Given the importance of high-quality big data for global scale studies, there is an urgent need for an improvement of the GNIR database.

Global map of stable isotopes in water is required for many hydrological, ecological and climatological applications. Bowen and Revenaugh [21] tested four interpolating methods and created a global map of interpolated isotopes in precipitation, and was applied to wildlife forensics [22]. Terzer et al. [23] produced an improved global prediction for isotopes in precipitation using regionalized climatic regression models, which is available from the IAEA website as Regionalized Climatic Water Isotope Prediction (RCWIP). Similar attempt was also conducted on isotopes in river water. Dutton et al. [24] generated a map of isotopes in river water across the conterminous USA using latitude and elevation as primary predictors. Bowen et al. [25] developed a geographic information system-based model to predict the river water isotopes in the contiguous United States. However, these works upon isotopes in river water were limited in regional scale because of the poor spatial coverage of available data.

A meta-analysis is a promising avenue in this respect. Actually, many water isotopic observations have been conducted in areas where no or few GNIR stations exist, such as the Nile [26], Western Europe [27] and the Tibetan Plateau [28]. Isotopic related studies have been also conducted in some hydrologically important regions, such as transboundary rivers [29], high mountainous regions [24] and high latitude regions [30]. Isotopic data in rivers can be found in these studies, thereby offering the potential for supplementing the GNIR database. In this study, we aim to present a wider-spread database with meta-analysis data extracted from published studies, and analyze the spatial pattern of

isotopic compositions in rivers on the basis of the extended database. A global map of river isotopes is generated as the benchmark for further researches on isotopic hydrology.

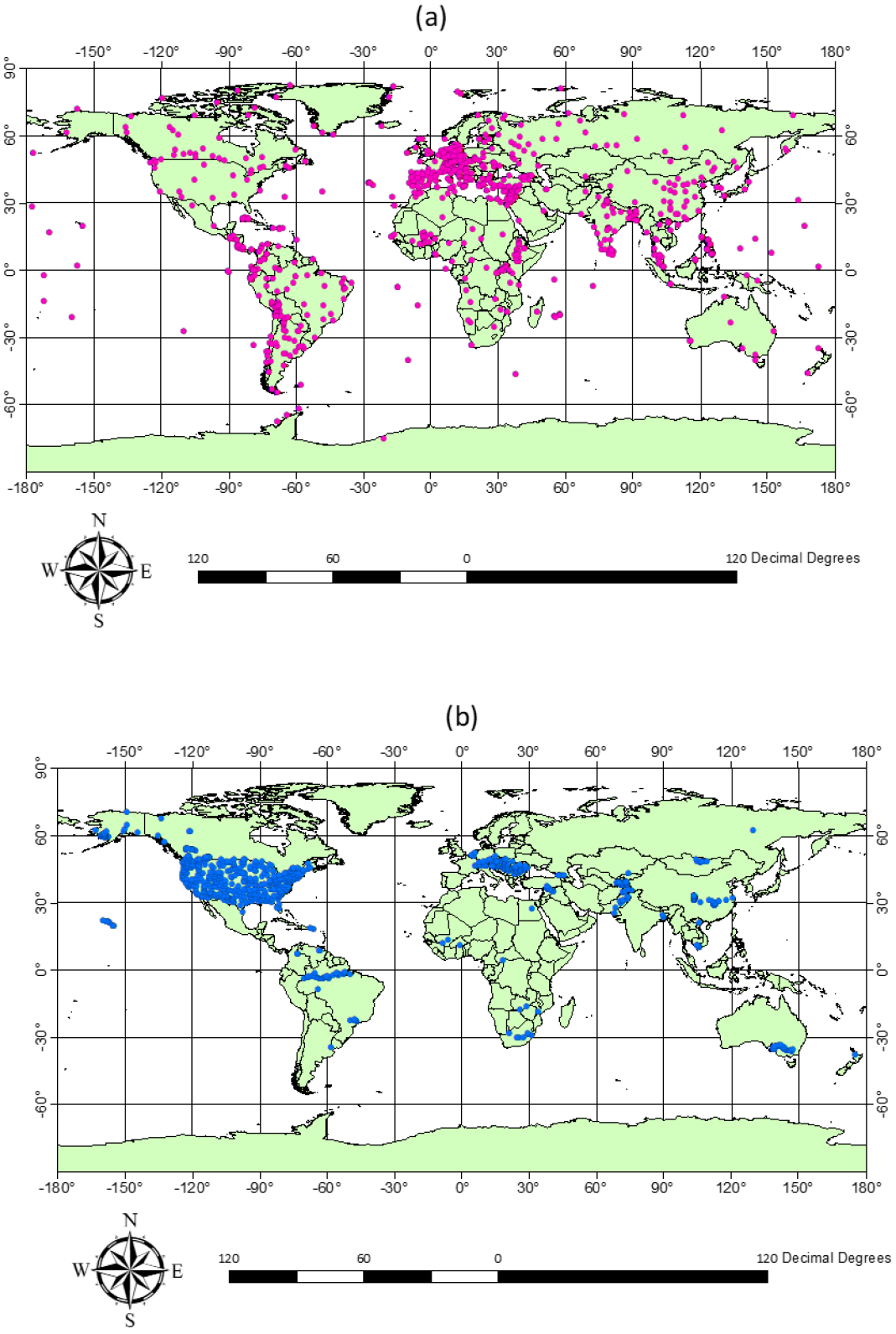

Figure 1. Distribution of data in GNIP (**a**) and GNIR (**b**) databases.

2. Data and Methodology

2.1. The GNIR Database

The GNIR is an online database launched in 2007 by the International Atomic Energy Agency (IAEA), complementary to the 45 years old GNIP database. Participation in GNIR is voluntary and stations are operated by hydrological services within the framework of national basin-scale observation networks, or by water research institutions and individual researchers, and even private citizens [19]. Three types of data are included in GNIR [31]: data from regularly monitored river stations with a sampling interval, instantaneous spatial profile-longitudinal surveys, and remaining ad-hoc data from previous IAEA Coordinated Research Projects and other scientific studies worldwide. GNIR data and statistics can be obtained free of charge from the Water Isotope System for Data Analysis, Visualization and Electronic Retrieval (WISER). Each of the GNIR data is comprised of four parts: river basin, sampling site, isotopic data at sampling site and other data such as river discharge and electrical conductivity. For more information of GNIR, the reader is referred to the IAEA website (https://nucleus.iaea.org/wiser).

2.2. Extension of GNIR Based on Literature Resources

Here, we propose to extend the GNIR database via a meta-analysis based on more than 1000 published papers extracted from Web-of-Science with the search keywords "isotope", "hydrology" and "river" as of March 2017. We retained a subset of 215 papers providing isotopic data suited for our subsequent analysis (a full list of the 215 papers can be found in the Supplementary Materials). These papers were published between 2004 and 2017. We noted a steep rise in publications between 2014 and 2016, showing the recent rise in interest and research made in this field (Figure S1). The 215 papers were mostly taken from top journals, which ensured the quality of the data (Figure S2). In all of these papers, isotopic data were reported in text, table, figure, and the type of water was indicated. To extend the GNIR database, we only selected the data which were corresponding to the water body type of "river", "stream" or "surface water", excluding some other common types such as "spring", "lake" or "precipitation". Original data records were preferred and surely collected in the database. Meanwhile, only statistical indices, such as mean, maximum and minimum values were available for a large portion of data (~7%). These indices were also helpful to understand the spatial pattern and build a global map, so they were collected into the database as well, with a note at the data record to explain the meaning of the indices. We contacted some of the authors for the original data to further supplement the database [32–35]. For the data in figure, the software GetData Graph Digitizer was used to extract the data. GetData Graph Digitizer [36] is a program for digitizing graphs and plots, which is helpful to obtain original "(x, y)" data from graphs. Supported graphics formats included TIFF, JPEG, BMP and PCX. Data can be extracted by simply setting the coordinate system and clicking the objective data point. The software can zoom the figure to the pixel size, which ensured the accuracy. The data were consequently classified into three types, i.e., original data, statistical indices, and data extracted from figures, which are labeled as one, two, three, respectively, by a tag variable.

In addition to the isotope data, we also collected spatial and temporal metadata. The original records of sampling location and time were preferred. However, exact sampling locations and time of sampling were not always available from the papers. For example, about half of the data had no accurate location information, a similar proportion of the data had a temporal resolution lower than daily, and only statistical values were obtained for a large portion of the data (~7%). In order to overcome this limitation, we used a coarse location/timing information where/when the research was conducted as a proxy. For spatial information, the average coordinates of the study region provided in studies or extracted from Google Earth or Wikipedia were adopted to obtain the sampling location. For temporal information, the most specific time range provided in the papers was used with a tag variable to describe the accuracy (i.e., one, two, three represent the time accurate to the day, month and wider range, respectively), which can represent the available temporal resolution

of the data. After adding the data extracted from our literature-based meta-analysis data, the GNIR database was significantly extended as shown in Figure 2. The new database is online available at http://www.thuwater.org/gnir-e, also available at Harvard Dataverse (doi:10.7910/DVN/XIJO5M).

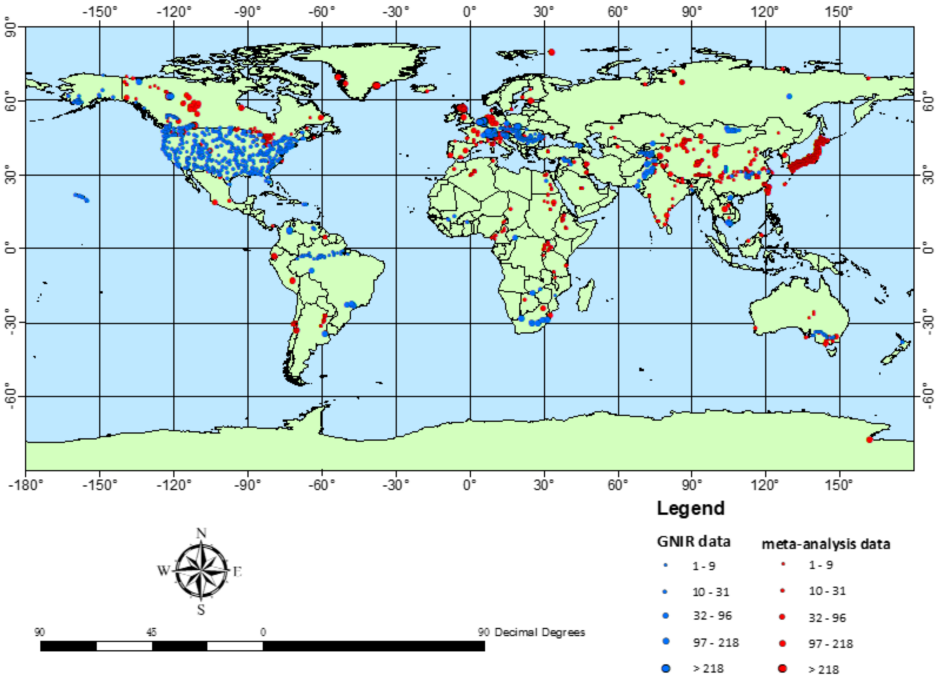

Figure 2. Location of GNIR data and meta-analysis data. Original GNIR data and meta-analysis are presented as blue points and red points, respectively. Sizes of the points represent amount of data.

2.3. Analysis on the Spatial Pattern of River Isotopic Data

With the extended isotope database, we carried out an analysis of the spatial patterns in river water isotope signatures. Relationships between δ^2H and $\delta^{18}O$ values, and between isotopic values and geographical or meteorological factors were analyzed using a statistical regression analysis. Here we chose the ordinary least squares regression (OLSR). OLSR is the most widely used regression to define the water line. Although different regression methods may result in different result [37], it is found that when a good linear relationship exists, different regressions result in similar fit [38]. When investigating the relationship between isotopic values and geographical or meteorological factors, OLSR is also the normally used regression method (e.g., Zhao et al. [15], Kendall et al. [13]). Besides, geographical and meteorological data are considered to have less error than isotopic data, so the OLSR is suitable because it assumes there is no error on x-axis [39].

Considering the potential difference among different regions, the data had to be divided into several groups prior to analysis. The regions were based on continents, and the completeness of land and the homogeneity of data distributions had to be ensured for each region. Consequently, the data was divided into six groups, i.e., Africa, Australia, China, Europe, North America and South America. Asia was not chosen as a region because of the inhomogeneous distribution of data in Asia, with regions such as Central Asia having a lot of data, while only extremely scarce data available in some other regions, such as the Middle East. Besides, Japan and Southeast Asia do not belong to the same mainland as other Asian areas. Covering a vast territory and having plenty of data with a dense spatial coverage, China was considered as a region.

To conduct the regression analysis, point-scale average isotopic values and meteorological/geographical data were determined. First, all of the locations collected from papers or GNIR were considered as a site. For the site with more than 5 isotopic measurements, the arithmetic average value of the data was used to represent the mean isotopic composition of this site. To take advantage of

integration of different data source, the sites with lower than 5 measurements were gathered into $1^\circ \times 1^\circ$ grids. For the gird with more than 5 measurements after integration, the arithmetic average value of data within this grid was used to represent the mean isotopic composition. Such grid was regarded as a site, and the center of grid was regarded as the location of the site. The subsequent analysis, including interpolation and regression were all based on the map of point-scale isotopic values.

The data used to run the regression model includes meteorological data, i.e., the global raster data of mean annual precipitation (MAP), mean annual temperature (MAT) [40], mean annual potential evapotranspiration (PET), aridity index (AI) [41,42] and mean annual relative humidity (RH) [43], and geographical data, i.e., latitude (LAT), longitude (LOG) and elevation (ELE) [44]. All the data were extracted to the site described above to represent the point-scale average condition for regression. First, we used LAT and LOG to describe the spatial patterns directly, deciding whether the distribution characteristics are significant according to the P value, which quantifies the idea of statistical significance of evidence [45]. In order to gain insights on the factors controlling the isotopic distribution patterns in each region, and to predict the river isotopes with meteorological and geographical data, the variables were combined in different permutations to conduct the multiple regression. The Akaike Information Criterion (AIC) was used to rank the model and to select the best predictors. The AIC balances the correlation coefficient and simplicity and can give an estimate of the quality of the regression model, which has a fundamental impact in statistical model evaluation problems [46]. The model with the minimum value of AIC is regarded as the best model which is the one with least complexity or highest information gain. In this work the corrected Akaike Information Criterion (AICc) Equation (1) was used because it is more applicable for the small samples [47].

$$AICc = AIC + \frac{2k(k+1)}{n-k-1} \quad (1)$$

where, k and n are the number of variables and samples, respectively, and AIC can be calculated by the AIC function in Matlab.

2.4. Global Interpolation of River Water Isotopes

A global map of river water isotopes was generated based on the extended isotope database. A water balance model based on geographic information developed by Bowen et al. [25] might be an alternative method to conduct such work. However, accurate spatial information of sample location was needed to get reasonable results, which is not available for about half of data points in our study. Therefore, we adopted the modelling approach of Dutton et al. [24], which was mainly based on the dependence of isotopes on environmental factors. Here, the best predictors for each region selected according to AICc rather than latitude and elevation, which was used in the study of Dutton et al., were used to establish empirical relation. The following process was done for each region: (1) determining the dependence of isotopes on the best predictors; (2) applying the empirical relation to the meteorological and geographical data based on these parameters; (3) mapping residuals between the regression model values and observed values; (4) adding model value map and residual map to generate a map of river isotopes for each region. Also, a global simplified interpolation using Kriging method was conducted to determine the values for the regions which were not analyzed for the best predictors as described in the previous section. After the regional maps were generated, they were merged together to get a global map.

3. Results

3.1. General Characteristics of the Improved Database

A total of 17,015 measurements of O and H isotopes in rivers have been collected (Table 1) and added to the original GNIR database that initially had 15,952 measurements (as of March 2017). Figure 2 shows that the spatial coverage has been significantly improved. Abundant information has been

added to areas with little or no data coverage in the original GNIR database, especially for China, Japan, Canada, Western Europe and Africa. As shown in Figure 3, the distribution of data along latitude and longitude is similar, but some regions are supplemented significantly, such as 20° W to 0°, 80° E to 100° E, 120° E to 180° E and 50° N to 80° N. For high latitudes, where sampling is extremely difficult, data were also extracted from literature, such as for Antarctica [48], Greenland [49] and pan-Arctic regions [30]. These new datasets provide a more complete picture of the global distribution of isotopic compositions in river waters. While the GNIR database has data since 1966, the time-series of added data is relatively short (Figure 4) because the studies selected in this research were all published after 2000. Nonetheless, the new database has more data after 2000, and thus can better represent the present isotopic characteristic of river waters.

Table 1. Key information of the meta-analysis database. The amounts of measurements of each temporal resolution and each data collection type are presented in the table.

Tag Variable	Value	Amount
Temporal Resolution [a]	1	9147
	2	2372
	3	5496
Data Type [b]	1	8000
	2	1204
	3	7811

[a] 1, 2 and 3 stand for temporal resolution of daily, monthly or longer time scale, respectively. [b] 1, 2 and 3 stand for data collected using original data in the articles, using statistical indices from the articles, or extracted from figures in the articles, respectively.

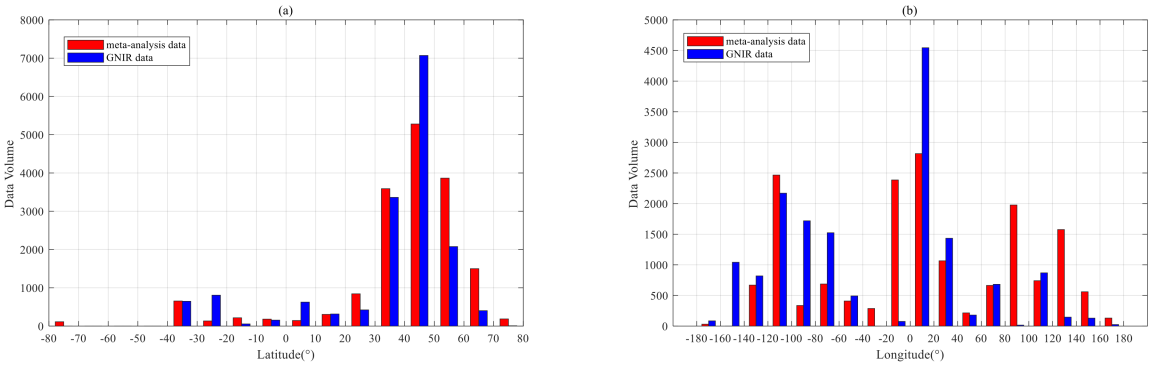

Figure 3. Data volume distribution of meta-analysis data and GNIR data along (**a**) latitude and (**b**) longitude.

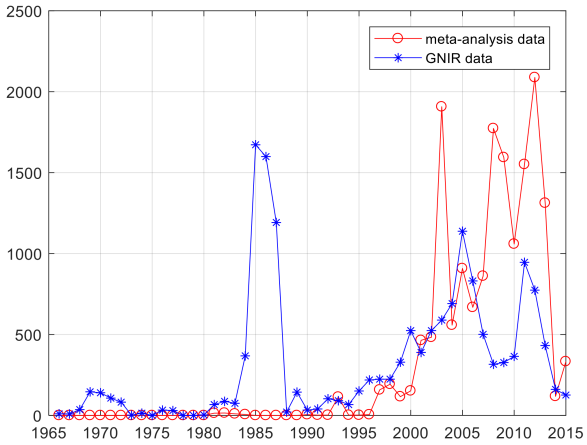

Figure 4. Time of GNIR data and meta-analysis data. Red circles and blue asterisks represent the amount of meta-analysis data and original GNIR data in the year, respectively.

3.2. Spatial Pattern of River Water Isotopes

The newly compiled database reveals a large range in $\delta^{18}O$ and $\delta^{2}H$ values in river water across the world. $\delta^{18}O$ varies from −42.3‰ to 14.75‰, with a mean value of −10.59‰. $\delta^{2}H$ varies from −340.85‰ to 58.84‰, with a mean value of −78.00‰. The Global River Water Line (GRWL) based on the 24,939 measurements (excluding the measurements missing either $\delta^{2}H$ or $\delta^{18}O$ data) in the compiled database is: $\delta^{2}H$ = 8.03 (±0.01) $\delta^{18}O$ + 8.59 (±0.13) (r^2 = 0.956) (Figure 5a) close to the relationship based on the original GNIR database: $\delta^{2}H$ = 8.09 (±0.01) $\delta^{18}O$ + 9.40 (±0.12) (r^2 = 0.977). The isotope data cluster plot near the Global Meteoric Water Line (GMWL: $\delta^{2}H = 8\delta^{18}O + 10$ [50], and the observed correlation based on the GNIP database: $\delta^{2}H$ = 8.14 (±0.02) $\delta^{18}O$ + 10.9 (±0.2) [51]), which indicates precipitation as an important source of river water. The distribution characteristics of the meta-analysis data are similar to that of the original GNIR data, but more meta-analysis data with $\delta^{18}O$ values are less than −20‰, which is a remarkable supplement that significantly expands the range of the GNIR dataset. It is also noteworthy that after adding the meta-analysis data, the isotopic distribution ranges of precipitation and rivers are more aligned, which is consistent with precipitation being the main source of river water.

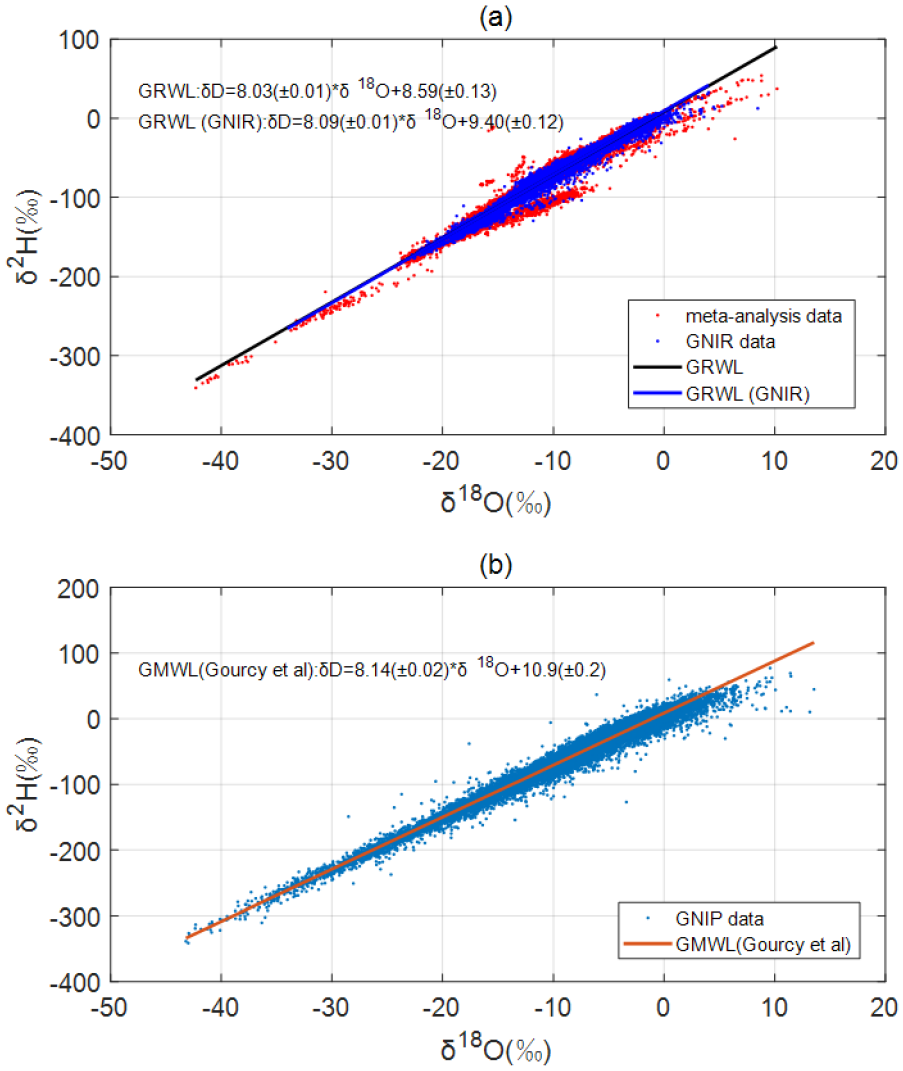

Figure 5. Relationship between $\delta^{18}O$ and $\delta^{2}H$ in river water (**a**) and precipitation (**b**) Points in red and blue in (**a**) represent meta-analysis data and original GNIR data, respectively.

The similarity between isotopes in river water and precipitation has been reported in many published papers [13,17]. However, isotopes in river water and precipitation are not the same in every respect. The distribution of the river isotope data appears asymmetric (Figure 5a)—best described as 'imbricate' (overlapping in sequence) by Kendall and Coplen [13], with river isotope distributions being significantly different from those in precipitation (Figure 5b). The slopes of $\delta^{18}O$-$\delta^{2}H$ relationship in precipitation and river water are also quite different within a same watershed. The HydroSHEDS data produced by Lehner and Grill [44] was used as the watershed boundaries. As shown in Figure 6, slopes of precipitation have a range of 5.6 to 8.8, while the range of slopes of river water is much wider (3.9 to 10.5). Figure 7 shows the global distribution of the difference between slopes of precipitation and river water. We can see that the watersheds where river line slopes are significantly lower than precipitation line are mainly distributed in Africa, Australia, Canada, North Europe, South and Southeast Asia. Such a distribution pattern can be partly attributed to the effect of evaporation. Most of the watersheds with large slope difference are located in the regions dominated by high potential evapotranspiration (e.g., Africa, Australia, South and Southeast Asia) or the regions influenced by lake (e.g., Great Slave lake and Athabasca lake in Canada, Lake Onega in North Europe). However, because the slope of river line is dependent on small-scale local processes or conditions [13], a good correlation between the slope with a single factor is hard to find.

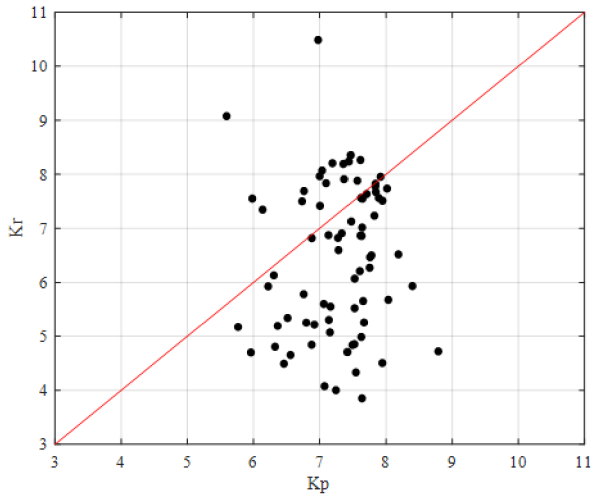

Figure 6. Slopes of $\delta^{2}H$-$\delta^{18}O$ relation in precipitation and river water. Kp and Kr stands for slope of $\delta^{2}H$-$\delta^{18}O$ relation in precipitation and river water, respectively. Each point represents Kp and Kr of a watershed. Red line is the 1:1 line.

The difference between isotopes in rivers and precipitation and the asymmetry of the river isotope dataset can be due to several factors. First, climatic conditions are different among regions, which can affect the isotopic composition and the slope during rainfall-runoff process. Second, river is a mixture of precipitation and other compositions, which can bring different isotopic composition to river water. Although other water bodies originate from precipitation as well, the isotopic composition may experience modification due to fractionation of different extent when phase transformation occurs (e.g., evaporation, transpiration, ice/snow formation and melting). Last, time scale also plays an important role because several processes cause mixing of waters with different ages. For example, preferential flow can result in young water infiltrating deeply into soils or rapidly contributing to streamflow or aquifers [52]. Moreover, canopy rainfall storage by vegetation can cause rainfall mixing with water retained from prior rain events [53]. Residence time of river water can be much older due to contributions of old groundwater during baseflow [54], which causes damped isotopic signal compared to precipitation [55].

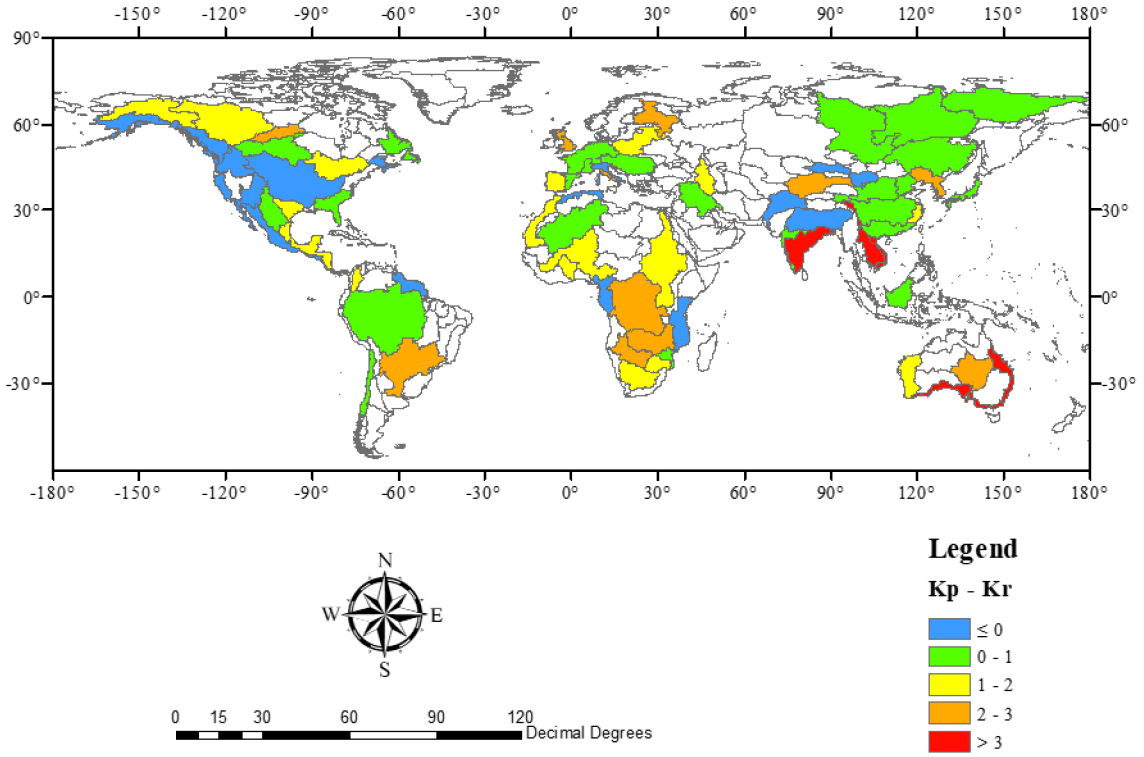

Figure 7. Global distribution of the difference between the catchment scale meteorological line and river line. HydroSHEDS data was used as the boundary of catchments. Blank regions indicate there are no sufficient data to calculate the slope of both lines.

Spatial patterns of the isotope values are analyzed using Moran's test [56] based on the point-scale average river isotope. Moran's I for δ^2H and $\delta^{18}O$ are 0.45 and 0.51, Z = 102.5 and 114.2, respectively ($p < 0.01$ for both), which means that the spatial distribution of river water isotopes is not random at global scale. Figure 8 shows the spatial distribution of mean values of river water isotopes, where individual point values are presented on the background colored using Kriging interpolation in ArcGIS 10.2. For comparison, the distribution of precipitation isotopes is shown in Figure 9. In general, the two datasets show an increasing depletion from equatorial regions to higher latitudes, as well as from coastal regions to inland regions in mainland areas such as Eurasia and North America. Such patterns in precipitation isotopes are described as 'latitude effect' and 'continental effect' [57]. These effects are mainly due to the spatial distribution of climatic conditions and distances to the moisture source [3]. Similar effects appear in the distribution of river isotopes because river is mainly sourced from precipitation. Differences also exist between the spatial patterns of isotope signatures in rivers and precipitation. The distribution of precipitation isotopes follows the latitude effect better, appearing as zonal background color on the map, while the river water isotopes have a seemingly more disordered distribution in some regions such as North America and China. This also indicates the complex influencing factors that could affect runoff generation and flow concentration processes in different regions.

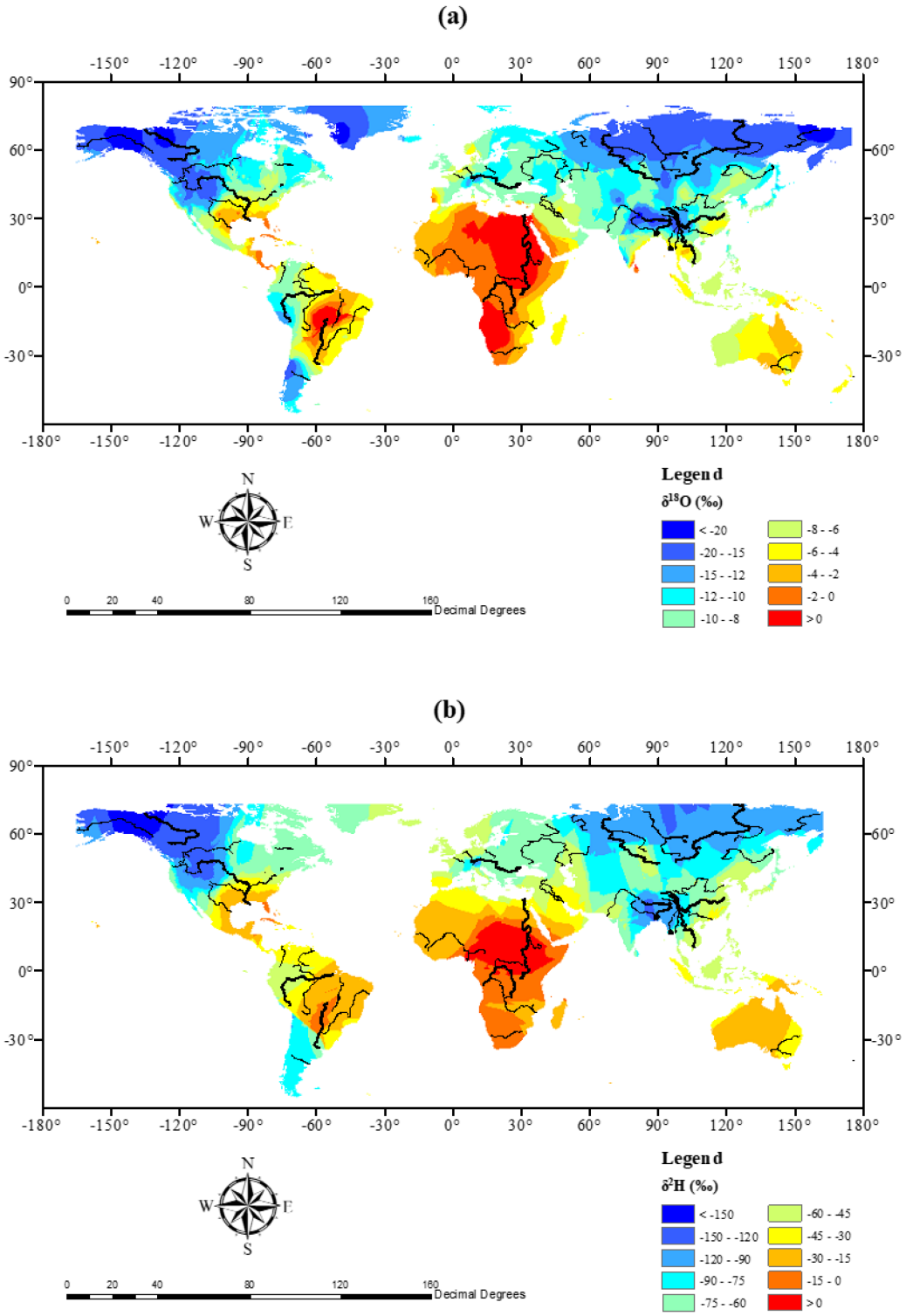

Figure 8. Global distribution of (**a**) $\delta^{18}O$ and (**b**) $\delta^{2}H$ in rivers. The values are overlaid on a background generated from Kriging interpolation model in ArcGIS 10.2. Black lines in the map are the major rivers [58].

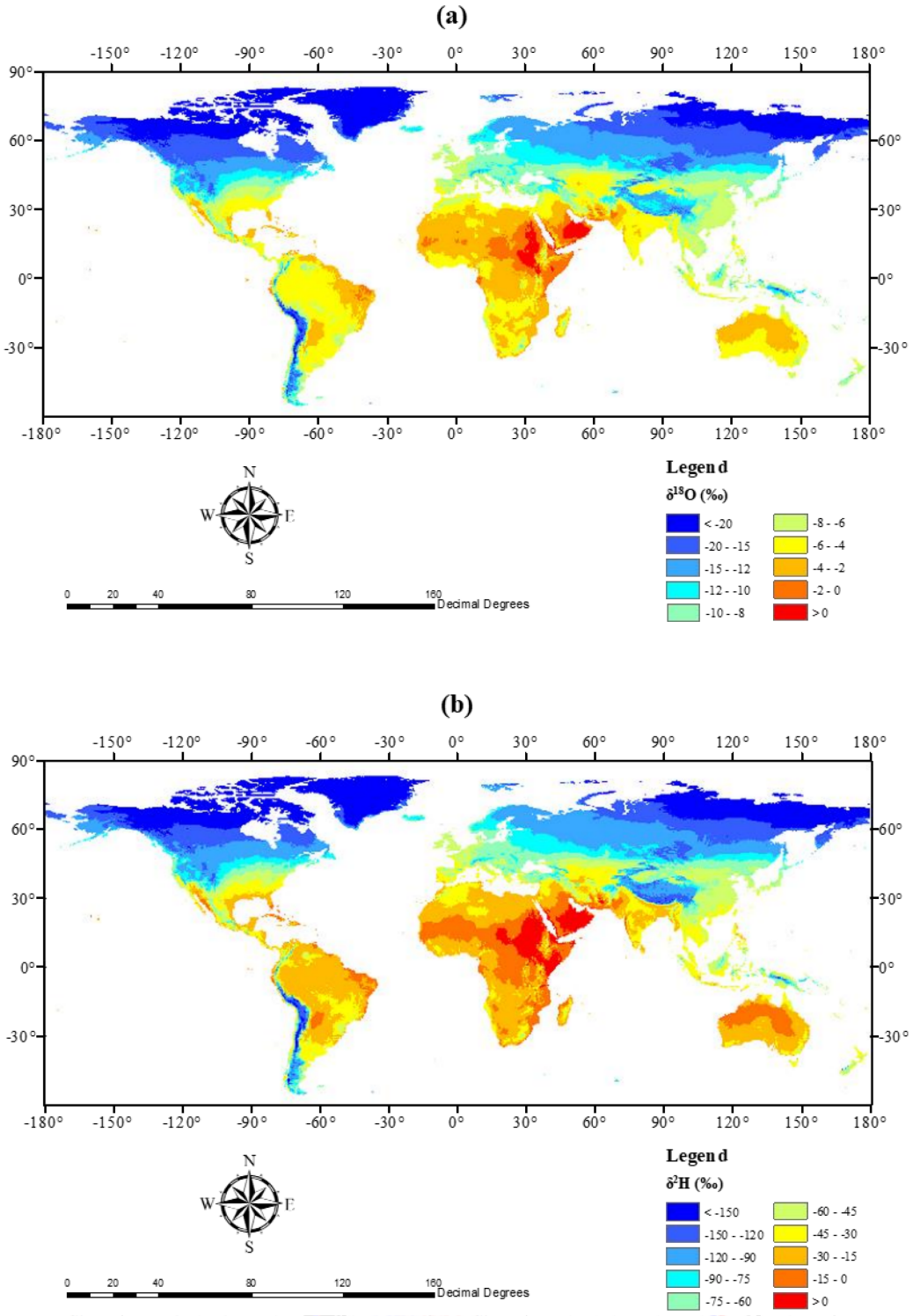

Figure 9. Global distribution of (**a**) $\delta^{18}O$ and (**b**) $\delta^{2}H$ in precipitation. The values are overlaid on a background based on Regionalized Climatic Water Isotope Prediction (RCWIP) [19,23].

4. Discussion

4.1. Relationship between $\delta^{18}O$ and $\delta^{2}H$ in River Waters

The Global River Water Line shows that the river isotope values do not converge along a single straight line. There are some branches that diverge from the main fitted line. This phenomenon suggests that different river water lines prevail in different regions. The relationships between $\delta^{2}H$ and

$\delta^{18}O$ in the six regions introduced in the methodology section are analyzed and the results are shown in Table 2 and Figure 10. For comparison, the results of precipitation isotopes calculated from the GNIP database are also presented. Different regions have similar Local Meteoric Water Lines (LMWL) with their slope comprised in the range of seven to eight, i.e., close to the GMWL $\delta^2H = 8\delta^{18}O + 10$). This complies with the anticipation that the LMWL will be close to GMWL once long-time series of dataset is used for analysis [59]. However, significant differences exist among each group of river water. In China, North America, Europe and South America, the Local River Water Lines (LRWL) are similar to the LMWLs, while in the other two regions the slopes of the LRWL are much lower than those of the LMWL. Low slopes of LRWLs are commonly associated with evaporation losses [15]. According to previous studies, the extremely low slope of the LRWL in Australia (~4.4) is a result of evaporation at an air humidity of around 50% [60].

Table 2. Relationship between $\delta^{18}O$ and δ^2H in precipitation and rivers in six regions. SA, AF, AU, EU, NA, CN represent South America, Africa, Australia, Europe, North America and China, respectively.

Water	Region	Result
Precipitation	SA	$\delta D = 7.88\ (\pm0.02) \times \delta^{18}O + 9.72\ (\pm0.14)$ $R^2 = 0.974$
	AF	$\delta D = 7.03\ (\pm0.03) \times \delta^{18}O + 8.12\ (\pm0.14)$ $R^2 = 0.920$
	AU	$\delta D = 7.20\ (\pm0.06) \times \delta^{18}O + 8.52\ (\pm0.28)$ $R^2 = 0.924$
	EU	$\delta D = 7.74\ (\pm0.01) \times \delta^{18}O + 6.13\ (\pm0.09)$ $R^2 = 0.971$
	NA	$\delta D = 7.88\ (\pm0.01) \times \delta^{18}O + 7.24\ (\pm0.21)$ $R^2 = 0.986$
	CN	$\delta D = 7.28\ (\pm0.05) \times \delta^{18}O + 3.97\ (\pm0.47)$ $R^2 = 0.925$
River	SA	$\delta D = 7.33\ (\pm0.03) \times \delta^{18}O + 3.51\ (\pm0.31)$ $R^2 = 0.974$
	AF	$\delta D = 5.66\ (\pm0.08) \times \delta^{18}O + 1.90\ (\pm0.27)$ $R^2 = 0.892$
	AU	$\delta D = 4.40\ (\pm0.12) \times \delta^{18}O - 9.69\ (\pm0.57)$ $R^2 = 0.770$
	EU	$\delta D = 7.82\ (\pm0.02) \times \delta^{18}O + 8.27\ (\pm0.23)$ $R^2 = 0.963$
	NA	$\delta D = 8.14\ (\pm0.01) \times \delta^{18}O + 6.50\ (\pm0.24)$ $R^2 = 0.954$
	CN	$\delta D = 7.22\ (\pm0.05) \times \delta^{18}O + 5.10\ (\pm0.60)$ $R^2 = 0.909$

Similar to the GRWL, the six LRWLs of each region also appear asymmetric, especially in Africa and North America, where two isotopic regression lines exist (Figure 10). To discuss the cause of bifurcation, the data points need to be classified into two subgroups based on δ^2H-$\delta^{18}O$ relation. The classification should follow two requirements. First, the data points at the same station (or extracted from the same paper) should be in the same group because of the similar hydrology processes. Second, the data points in a group should cluster well around a line, meanwhile the line of two groups should be significantly different. The data points near the intersection of two lines are difficult to group, while the data points far from the intersection are easy to identify. Consequently, the data in the range far from intersection (i.e., −10‰ to −5‰ for North America and larger than 0‰ for Africa) were picked out to derive two different regression lines using least-squares fitting approach. Mean differences of data at each station (or from each paper) from the two lines were calculated and compared to determine which group the data should belong to.

Consequently, the data in these two regions can be divided into two groups (Figures 11 and 12). In Africa, the groups with low and high slopes are located in the western and eastern part of Africa, respectively. This pattern can be explained, to some extent, by the distribution of evaporation. According to the PET data, Africa is dominated by high evaporation, which makes the slopes of both groups much lower than 8. The obvious difference between the two groups is the climate of the river source region. In Group 1, the data points mainly distribute in the Nile River Basin. The two main tributaries, i.e., White Nile and Blue Nile, source from Rwanda and Lake Tana in Ethiopia, respectively. According to Figure 10a, the potential evapotranspiration of these source regions is relatively low, leading to a higher slope. In Group 2, the data points are mainly distributed across the Niger River Basin, sourcing from the Guinea Highlands, where evaporation demand is intensive, causing the slope of the LRWL extremely low. Other data points in Group 2 are distributed in South Africa along

Zambesi River. According to the original papers, the data in South Africa were sampled at rivers effected by lake or wetland (e.g., Lake Ngami [61], Mohlapitsi Wetland [62]), which causes significant evaporation losses because of the wide water surface. In North America, data points in Group 2 are mainly located near the continental divide, but only in the Northern US and Canada. As reported in previous work [13], the samples with relatively low local slopes are mainly distributed in the Western US, and the distribution exhibits correlation with topography or physiographic region. In Canada, the data in Group 2 are mainly located at rivers effected by lakes, which are also reported in some of data source papers (e.g., North Alberta effected by Mildred Lake [63], Baker Creek effected by Pocket Lake [64]). These data with low local slopes consequently form a line with low slope on a continental scale. But it should be noticed that the slopes of local line are not always consistent with the slope of continental line. As an example, the local slope of Cross river is 8.63, but the data belong to Group 2. Another exception is that the stations in Southwestern US generally have low local slope, but they belong to Group 1. This indicates complex influence factors on the large-scale river water lines, including both local processes and the spatial pattern of isotope compositions. Nonetheless, as evaporation processes are the most significant modification on isotopes in rivers, the difference between isotopes in precipitation and rivers should exist on all continent and their visibility depend on the available data. Further work and more data are needed to better understand the difference of LRWLs among rivers, watersheds or regions.

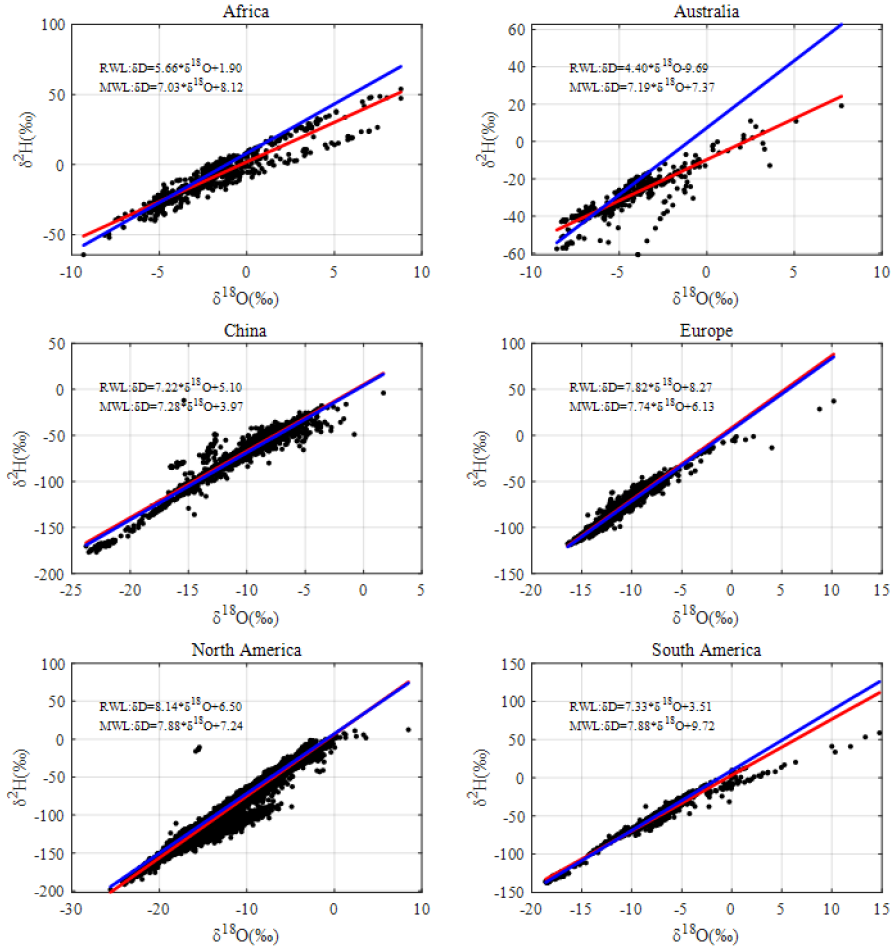

Figure 10. Relationship between $\delta^{18}O$ and $\delta^{2}H$ in river water in six regions. Black points represent the $\delta^{2}H$-$\delta^{18}O$ data points. Lines in red and blue represent the river and meteoric water line (RWL and MWL) of the regions, respectively.

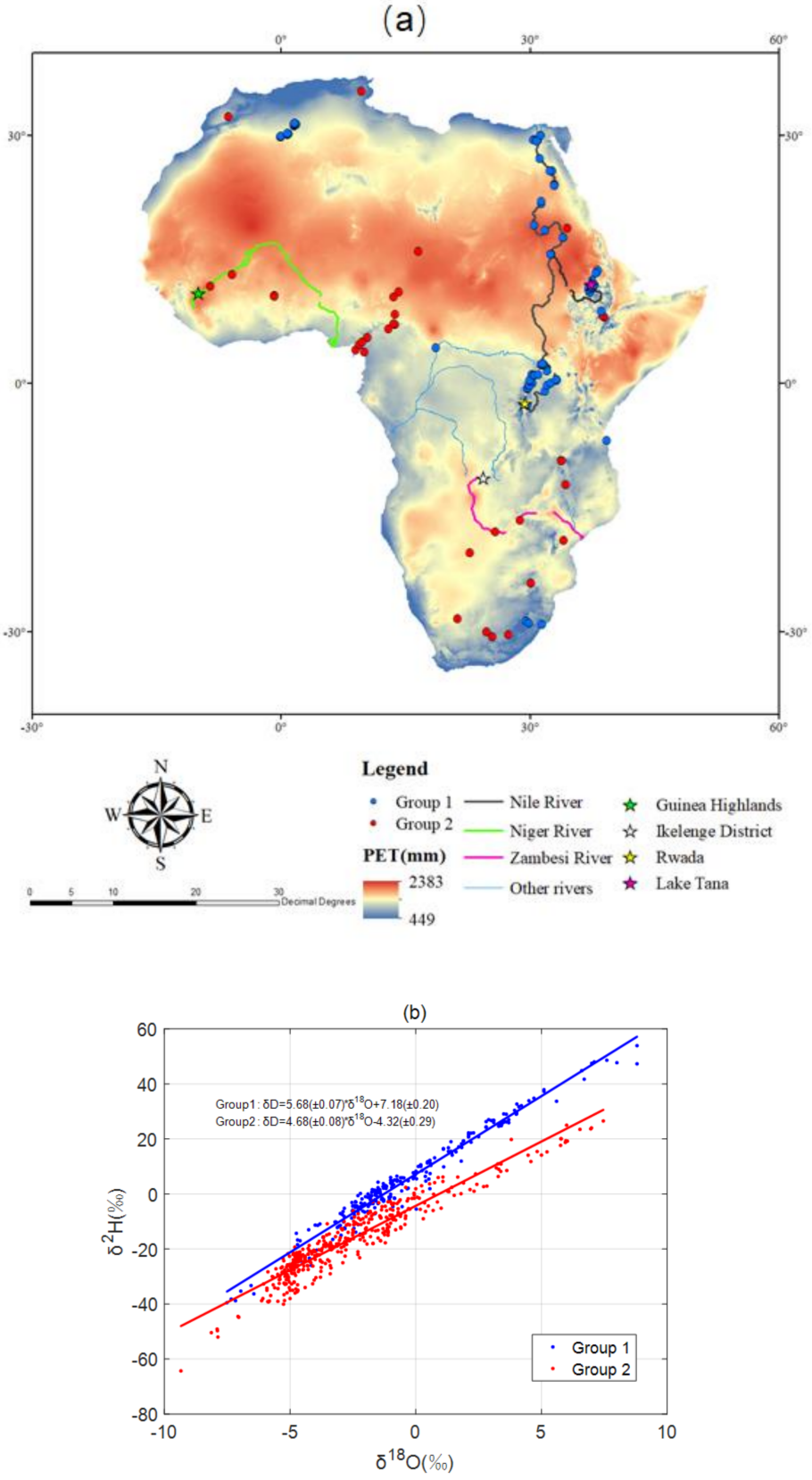

Figure 11. Group of isotopic data in Africa. (**a**) Location of data points in Africa. (**b**) ^{2}H-$\delta^{18}O$ relationship in Africa. Blue and red points stand for data points with high and low slopes, respectively. Background of (**a**) is the annual potential evapotranspiration (PET) data from CGIAR-CSI [41,42]. Lines in the map are the major rivers in Africa according to Naturalearthdata [58]. Stars in the map represent the source regions of Niger, Nile and Zambezi.

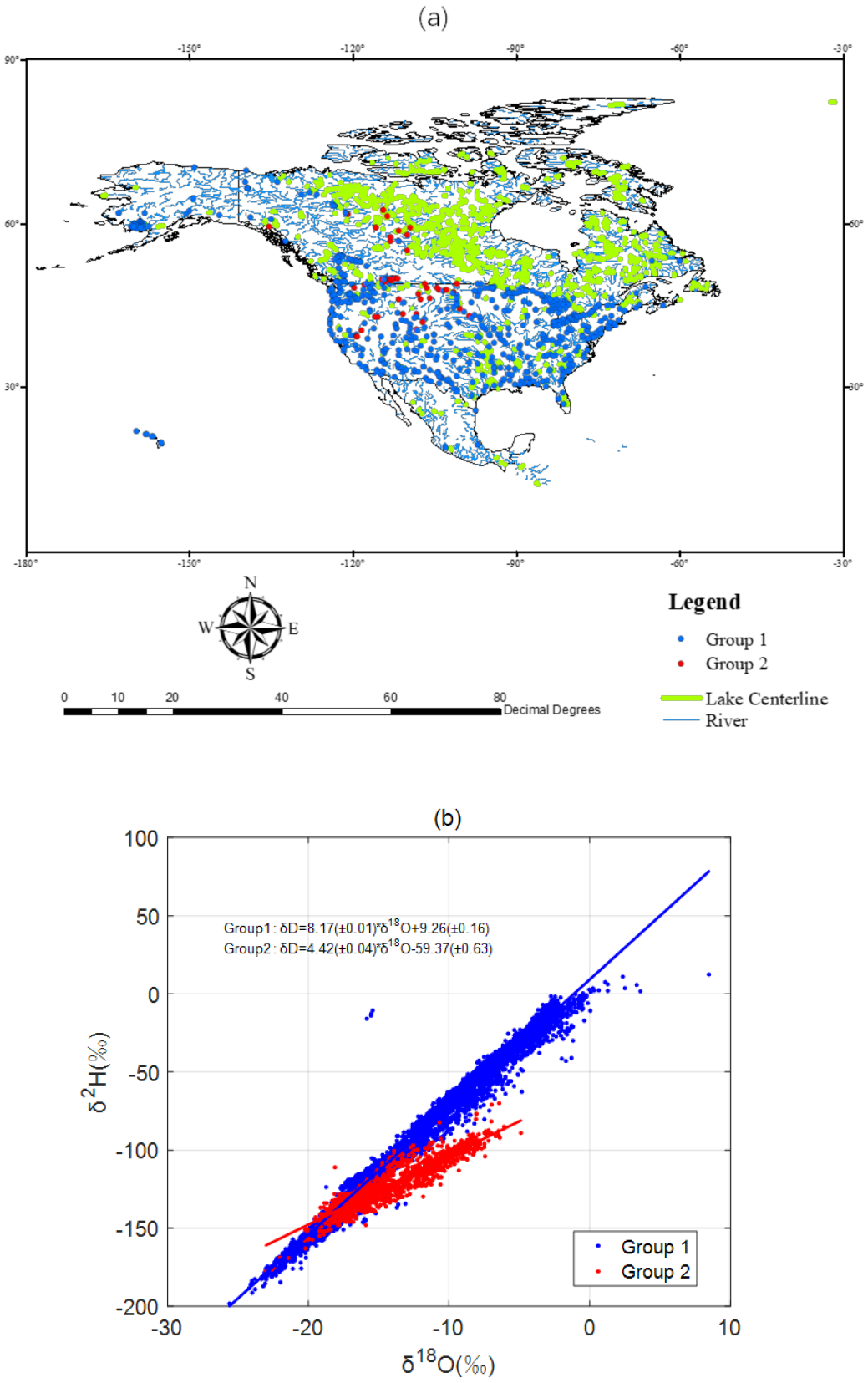

Figure 12. Group of isotopic data in North America. (**a**) Location of data points in North America. (**b**) ^{2}H-$\delta^{18}O$ relationship in North America. Blue and red points stand for data points with high and low slopes, respectively. Blue and green lines in the map are the major rivers and lake centerlines in North America, respectively [58].

4.2. Correlations between River Water Isotopes and Geographical Factors

Given that the spatial distribution of river water isotopes has specific patterns as shown in Figure 7, the coordinates of data points are used to quantify the pattern. For comparison, the same work is also conducted on precipitation isotopes based on the GNIP data. The data are divided into several groups like in the previous section but with some revisions. First, each group of data must have a wide spatial range so that a reasonable regression with geographical factors can be obtained. Australia is excluded from the calculation due to poor spatial coverage. Besides, considering the pattern in two hemispheres cannot be expressed in only one equation because of the different signs of the latitude, the regions crossing the equator (Africa and South America) should be divided into two parts. Last, a minimum amount of data is needed for the calculation of the regression, so that the regions with limited data (<10) are excluded: the northern part of South America. Given that $\delta^{18}O$ and $\delta^{2}H$ have similar spatial patterns, we only chose here $\delta^{18}O$ to implement the regression.

Table 3 shows the fitted coefficient of latitude and longitude and r^2 for the regression. For precipitation, the 'latitude effect' is well reflected for mid and high latitude regions (China, North America and Europe). However, in low latitude regions near the equator, there is no significant correlation between isotope values and latitude, and a significant correlation between isotope values and longitude can be found in South America instead. The 'latitude effect' is mainly a result of the distribution of climate characteristics and distance from the moisture source. However, in low latitude regions near the equator, it is close to the moisture source, and the climatic factors change relatively indistinctively along latitude, so that there is no significant 'latitude effect'. The correlation with longitude in South America indicates the east-west direction change of moisture composition, and the influence of Andes mountain could be another factor.

Table 3. Result of the regression analysis. Values in 'Lat' and 'Log' columns represent the fitted coefficient of latitude and longitude. The symbols *, ** and *** indicate statistical significance at the significance level of 0.05, 0.01, 0.001, respectively. Values in 'R^2' columns represents the r^2 values for the regression.

	Region	Result		
		Lat	Log	R^2
Precipitation	AF (N)	−0.062 **	0.007	0.150
	AF (S)	0.039	0.041	0.164
	SA (S)	0.059	0.160 ***	0.110
	EU	−0.207 ***	−0.072 ***	0.495
	NA	−0.506 ***	−0.022	0.827
	CN	−0.231 ***	0.072 *	0.441
River	AF (N)	0.017	0.139 ***	0.600
	AF (S)	0.087	−0.477 ***	0.607
	SA (S)	0.193 *	0.383 ***	0.435
	EU	−0.001	−0.043 *	0.030
	NA	−0.315 ***	0.026 ***	0.555
	CN	0.319 ***	0.184 ***	0.392

For river water, conditions are similar in South America and North America, which indicates the dominant role of precipitation on river water in these regions. According to the study of Kendall and Coplen [13], river samples can be used as proxies for average rain composition in the US, this finding may also be applicable in South America because of the similar significance and value of parameters between precipitation and river water. However, it is quite different in Africa and China. A significant correlation between river isotope and longitude exists in both North and South parts of Africa. Three large river catchments, i.e., Niger River, Congo River and Nile River distribute along the west-east direction, thus the correlation with longitude can reflect the significant difference among these catchments. In China, according to the regression result, $\delta^{18}O$ values have positive correlations with both latitude and longitude. The positive correlation with latitude may violate the 'latitude effect'. The 'anti-latitude effect' occurring in China could be due to two factors. First, high altitudes can lead to

extremely light isotopes in precipitation and surface water as a result of the strong negative correlation between isotopic signatures and altitude [65]. In southwestern China, altitudes are extremely high because of the Tibetan Plateau. However, there are few GNIP data points in the western part of China with high latitude, thus the positive correlation between isotopes and latitude may not be identified when carrying out the regression by only using GNIP data. That's why the result of precipitation does not show the 'anti-latitude effect'. Second, the r^2 of the regression with longitude (0.19) is much higher than that with latitude (0.02), indicating that longitude is the major control factor on river isotopes in China. This result is coherent with the fact that the major rivers in China are almost all flowing from west to east, which could cause the change in isotopes along longitude. The regression model with latitude and longitude is not suitable to describe the distribution of river isotopes in Europe as indicated by the low r^2, which may be a result of the East-west and North-South trending mountain ranges and rivers, respectively. Generally, the correlation coefficients of multiple regressions are relatively low when only using latitude and longitude, especially in Europe.

4.3. Correlations between River Water Isotopes and Meteorological Factors

As discussed in the above section, spatial patterns of river water isotopes are different in different regions (the north part of South America is excluded because of the little data quantity). Meteorological factors are used to build the regression model and gain insights on the controlling factors in each region. The models with highest *AICc*, which are regarded as the best models, are listed in Table 4. The variables in bold font are the behavioral variables used in more than three of the top five models in the region, which are considered to be the main controlling factors or best predictors of the distribution pattern. After using meteorological data, the performance of regression models is significantly improved. The r^2 values are all larger than 0.5.

Table 4. Summary of the result of regression models. The equation, *AICc* and r^2 of the best regression models of each regions are listed in the table. The bold font represents the behavioral variable which is defined as being used in more than 3 of the 5 top regression models.

Region	Equation [a]	AICc	r^2
Africa (North)	$\delta^{18}O$ = 0.167 (±0.017) **LOG** −41.8 (±7.52) AI +0.021 (±0.004) PPT −1.26 (±0.48)	6.47	0.89
Africa (South)	$\delta^{18}O$ = −0.885 (±0.136) **LOG** +0.256 (±0.062) **RH** +7.27 (±1.97)	9.20	0.78
Australia	$\delta^{18}O$ = −0.007 (±0.003) **PET** * −0.008 (±0.002) **PPT** +8.63 (±4.58)	17.00	0.50
China	$\delta^{18}O$ = 0.096 (±0.038) **LAT** −0.002 (±0.0002) **ELE** −0.008 (±0.001) **PET** * −1.95(±2.32)	190.69	0.57
Europe	$\delta^{18}O$ = −0.033 (±0.013) LOG +0.096 (±0.027) **LAT** * +0.375 (±0.021) **MAT** −17.1 (±1.39)	68.58	0.65
North America	$\delta^{18}O$ = −0.878 (±0.036) **LAT** −0.006 (±0.0002) **ELE** −0.611 (±0.047) **MAT** +35.4 (±2.01)	641.12	0.82
South America (South)	$\delta^{18}O$ = −0.010 (±0.004) PET +1.248 (±0.199) **MAT** −0.008 (±0.002) **PPT** −4.30 (±4.34)	89.46	0.77

* The parameter is recognized as behavioral, but the coefficient is against the regular patterns as "latitude effect" and "evaporation effect". [a] LOG: longitude (°), LAT: latitude (°), AI: aridity Index, PPT: mean annual precipitation (mm), PET: mean annual potential evapotranspiration (mm), MAT: mean annual temperature (°C), RH: relative humidity (%).

The best models and predictors in different regions are also quite different, and some regular patterns can be found. First, in six of the seven regions, coordinates (latitude or longitude) are used in the best regression model, among which it is the best predictor in four of the regions (both parts of Africa, Europe and North America). Coordinates reflect several factors such as distance from the moisture source and temperature, which have a strong effect on isotopes. This regression model therefore performs well in predicting the spatial patterns. The good performance of the coordinates-based regression model relates to the significant influence of water source on rivers. The poor behavior of coordinates in Australia could attributed to the small spatial range of data. Second, the variables including elevation, temperature, precipitation and evaporation play important roles in all of the regions. The effects of these variables on precipitation isotopes have been widely reported in previous studies, i.e., "altitude effect", "temperature effect", "amount effect" and "evaporation effect" [3,13,64], and the similar effect on river water also indicates the precipitation being main source of river water. While other factors, i.e., aridity index and relative humidity, do not work well in most of the regions. Thirdly, the signs of the coefficients do not always consist with the general effect described above. For example, the isotopic composition should increase with temperature, but the coefficient of temperature in North America is −0.611, less than zero. However, for most of the behavioral variables, the signs consist with the effect, which can reflect the effect of environmental factors on isotopes. The exception is latitude in Europe ($0.096 > 0$) and potential evapotranspiration in China ($-0.008 < 0$) and Australia ($-0.007 < 0$). The positive coefficient of latitude in Europe is mainly due to the distribution of samples. The samples in Europe are mainly distributed along the Rhine and Danube. Rhine flows from south to north thus the samples along Rhine cause the spatial variability along latitude, and the positive correlation is a result of isotopic enrichment due to evaporation along the flow path. In China and Australia, the positive correlation between isotope and potential evapotranspiration can be identified as expected when the simple linear regression is conducted. But when the variables are combined, the correlations with a single variable are not always same with that of simple regression because they are not independent with each other. Lastly, some single variables which have good correlations with isotopes may not perform well when multiple regressions are conducted, which is also a result of interactive effects. For example, in China, river isotopes have relatively well correlated with temperature, with r^2 value of 0.27, which is larger than that of evaporation (0.096), but the model with temperature is only the second top model of the region, and temperature is not a behavioral variable like evaporation. This is due to the strong linear relationship between temperature and evaporation ($r^2 = 0.70$), which makes temperature unnecessary to improve the performance of the model on the basis of evaporation. This might be a disadvantage of the multiple regression method. To reach the best simulation result, the regression equation may loss physical mechanism.

Based on the best predictors and regression models, a global map of isotopes in river water is generated (Figure 13). This map is similar with the Kriging map to some extent, but it can better describe some local pattern in regions with few data points because of the application of relationship between isotopes and other parameters. Comparing with the simple Kriging map, the regression-based map can better describe the low isotopic value in Andes Mountain, and the south-north direction decrease tendency in Australia, as reflected in the RCWIP map. Another two notable differences between two maps are in Brazil and Patagonia. The Kriging method produces high values of $\delta^{18}O$ in central Brazil and lower values in coastal regions but the pattern is reversed in the regression map. Similarly, the Kriging method produces low values in Patagonia but the regression method produces a west-east direction increasing trend. As previous studies have indicated that river isotopic compositions can preserve large-scale isotopic signatures in precipitation [13] and the RCWIP allows for an a priori prediction of isotopic composition in rivers [17], the similar pattern produced by RCWIP map (i.e., the higher values in central Brazil than coastal regions and the west-east direction increasing trend in Patagonia) may indicate better behavior of regression map than Kriging map in some regions.

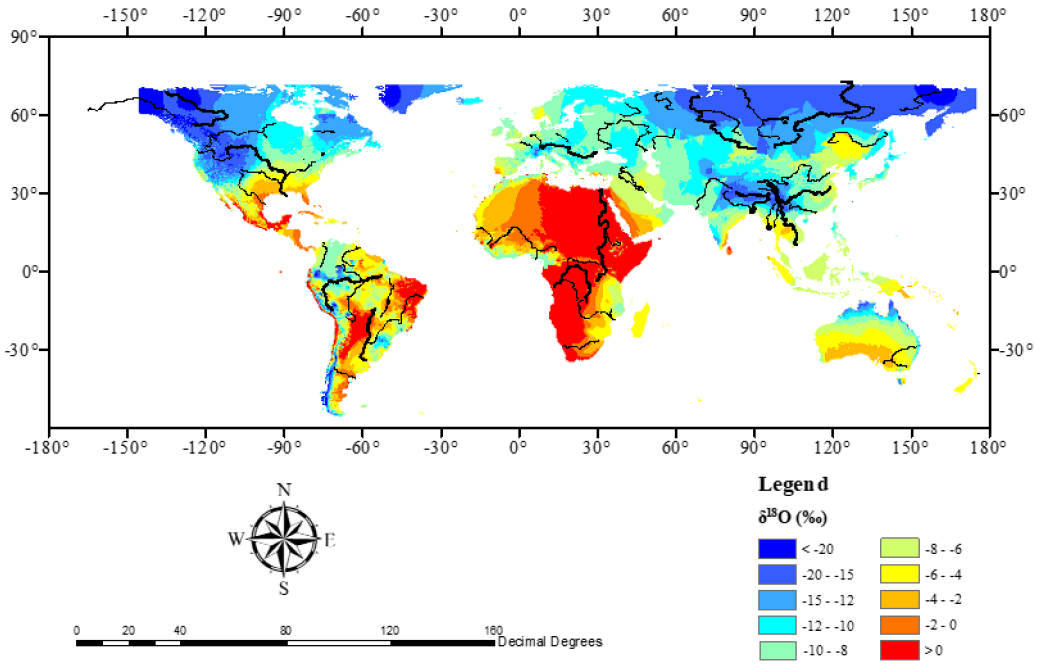

Figure 13. Global map of $\delta^{18}O$ in rivers. The values are overlaid on a background generated by regression-based interpolation method. Black lines in the map are the major rivers [58].

But the regression map also has its limitation. First, it might magnify the spatial variability in the regions where the spatial coverage of data is poor such as Australia, because the value within the whole continent will be determined by the data within a much smaller region. Second, the regression analysis is conducted in each region separately, and the global map is an integrate generated by splicing regional maps together, so there might be discontinuity values at the boundary among regions, i.e., China and the surrounding region, the equatorial zone in Africa. This is just a first attempt to map the global isotopic pattern of river water, and a primary benchmark for further research on river isotopes is established. More data are needed to verify and develop this map.

5. Conclusions

This study is the first attempt to provide a global coverage of river isotopes building on the GNIR database and a meta-analysis method by collecting isotopic data in rivers from published articles. It provides an unprecedented opportunity to analyze the global distribution features of stable isotopes in river waters. The results demonstrate that the pattern of isotopes in rivers is significantly different from that of precipitation. The relationship between $\delta^{18}O$ and $\delta^{2}H$ appears asymmetric, different from the flatter ellipse produced by isotopes in precipitation. Bifurcation of LRWL can be observed in Africa and North America, indicating the effect of evaporation, especially the evaporation of wide water surface in lake or wetland system. Based on a multiple regression model with geographical factors, spatial patterns of isotopes are different in different regions. Using meteorological data, a regression model can well predict the distribution of river isotopes, but the best models and predictors are different among regions. This work presents the first global river isotope map and establishes a benchmark for further research on isotopes in river.

Although the GNIR database is significantly improved, there are still regions with few data (e.g., Russia, the northern Australia). The results presented in this paper are quite speculative because they are extremely dependent on the available data, which is the most significant shortage of this work, and more data are needed to provide a more complete knowledge of isotopes in river across the word.

Supplementary Materials: The following are available online at http://www.mdpi.com/2073-4441/11/9/1760/s1, Figure S1: The number of publications on river isotopes that satisfied our criteria from 2001 to 2017, Figure S2: The source journals on which river isotope data were published, Information of data source.

Author Contributions: Y.N. organized the data collection and drafted the initial manuscript. F.T. and H.H. proposed the design for data collection. L.W. proposed the global interpolation of isotopic maps. All authors edited and reviewed the manuscript.

Funding: This study was supported by the National Science Foundation of China (91647205), and the Ministry of Science and Technology (2016YFC0402701, 2016YFA0601603). LW acknowledges partial support from the Division of Earth Sciences of National Science Foundation (NSF EAR-1562055 and 1554894) and the President's International Research Awards from Indiana University.

Acknowledgments: The authors would like to acknowledge all the cited authors (the detailed list is provided in the supplementary materials) for conducting the researches and providing isotopic data. We also would like to thank Dexin Li and Xiaoyang Zhong from Tsinghua University for the contribution in extracting data from articles. Arrangements to obtain the dataset can also be made by contacting the corresponding author (tianfq@tsinghua.edu.cn).

Conflicts of Interest: The authors declare no competing interests.

References

1. Gat, J.R. Oxygen and hydrogen isotopes in the hydrologic cycle. *Annu. Rev. Earth. Planet. Sci.* **1996**, *24*, 225–262. [CrossRef]
2. Bowen, G.J.; Cai, Z.; Fiorella, R.P.; Putman, A.L. Isotopes in the water cycle: Regional-to global-scale patterns and applications. *Annu. Rev. Earth Planet. Sci.* **2019**, *47*, 453–479. [CrossRef]
3. Dansgaard, W. Stable isotopes in precipitation. *Tellus* **1964**, *16*, 436–468. [CrossRef]
4. Zhao, L.; Xiao, H.; Zhou, M.; Cheng, G.; Wang, L.; Yin, L.; Ren, J. Factors controlling spatial and seasonal distributions of precipitation δ18O in China. *Hydrol. Process.* **2012**, *26*, 143–152. [CrossRef]
5. Wang, L.; Niu, S.; Good, S.P.; Soderberg, K.; McCabe, M.F.; Sherry, R.A.; Luo, Y.; Zhou, X.; Xia, J.; Caylor, K.K. The effect of warming on grassland evapotranspiration partitioning using laser-based isotope monitoring techniques. *Geochim. Et Cosmochim. Acta* **2013**, *111*, 28–38. [CrossRef]
6. West, A.G.; February, E.C.; Bowen, G.J. Spatial analysis of hydrogen and oxygen stable isotopes ("isoscapes") in ground water and tap water across south Africa. *J. Geochem. Explor.* **2014**, *145*, 213–222. [CrossRef]
7. Goldsmith, G.R.; Allen, S.T.; Braun, S.; Engbersen, N.; González-Quijano, C.R.; Kirchner, J.W.; Siegwolf, R.T. Spatial variation in throughfall, soil, and plant water isotopes in a temperate forest. *Ecohydrology* **2019**, *12*, e2059. [CrossRef]
8. Jasechko, S.; Kirchner, J.W.; Welker, J.M.; Mcdonnell, J.J. Substantial proportion of global streamflow less than three months old. *Nat. Geosci.* **2016**, *9*, 126. [CrossRef]
9. Jasechko, S.; Sharp, Z.D.; Gibson, J.J.; Birks, S.J.; Yi, Y.; Fawcett, P.J. Terrestrial water fluxes dominated by transpiration. *Nature* **2013**, *496*, 347. [CrossRef]
10. Evaristo, J.; Jasechko, S.; Mcdonnell, J.J. Global separation of plant transpiration from groundwater and streamflow. *Nature* **2015**, *525*, 91. [CrossRef]
11. Sprenger, M.; Tetzlaff, D.; Buttle, J.; Laudon, H.; Leistert, H.; Mitchell, C.P.; Snelgrove, J.; Weiler, M.; Soulsby, C. Measuring and modeling stable isotopes of mobile and bulk soil water. *Vadose Zone J.* **2018**, *17*. [CrossRef]
12. Berry, Z.C.; Evaristo, J.; Moore, G.; Poca, M.; Steppe, K.; Verrot, L.; Asbjornsen, H.; Borma, L.S.; Bretfeld, M.; Seyfried, M.; et al. The two water worlds hypothesis: Addressing multiple working hypotheses and proposing a way forward. *Ecohydrology* **2017**, *11*, e1843. [CrossRef]
13. Kendall, C.; Coplen, T.B. Distribution of oxygen-18 and deuterium in river waters across the United States. *Hydrol. Process.* **2001**, *15*, 1363–1393. [CrossRef]
14. Liu, J.; Song, X.; Yuan, G.; Sun, X.; Yang, L. Stable isotopic compositions of precipitation in China. *Tellus Ser. B Chem. Phys. Meteorol.* **2014**, *66*, 39–44. [CrossRef]
15. Zhao, S.; Hu, H.; Tian, F.; Tie, Q.; Wang, L.; Liu, Y.; Shi, C. Divergence of stable isotopes in tap water across China. *Sci. Rep.* **2017**, *7*, 43653. [CrossRef] [PubMed]
16. Xiao, W.; Fu, J.; Wang, W.; Wen, X.; Xu, J.; Xiao, Q.; Li, X.; Hu, C.; Liu, S. Estimating evaporation over a large and shallow lake using stable isotopic method: A case study of Lake Taihu. *J. Lake Sci.* **2017**, *29*, 1009–1017.

17. Halder, J.; Terzer, S.; Wassenaar, L.I.; Araguásaraguás, L.J.; Aggarwal, P.K. The global network of isotopes in rivers (GNIR): Integration of water isotopes in watershed observation and riverine research. *Hydrol. Earth Syst. Sci.* **2015**, *19*, 3419–3431. [CrossRef]
18. Wei, Z.; Lee, X.; Aemisegger, F.; Benetti, M.; Berkelhammer, M.; Casado, M.; Xiao, W.; Wright, J.S.; Wen, X.; González, Y.; et al. A global database of water vapor isotopes measured with high temporal resolution infrared laser spectroscopy. *Sci. Data* **2019**, *6*, 180302. [CrossRef]
19. IAEA/WMO. Global Network of Isotopes in Precipitation. The GNIP Database, 2019. Available online: https://nucleus.iaea.org/wiser (accessed on 5 March 2017).
20. Kaseke, K.F.; Wang, L.; Wanke, H.; Turewicz, V.; Koeniger, P. An analysis of precipitation isotope distributions across Namibia using historical data. *PLoS ONE* **2016**, *11*, e0154598. [CrossRef]
21. Bowen, G.J.; Revenaugh, J. Interpolating the isotopic composition of modern meteoric precipitation. *Water Resour. Res.* **2003**, *39*. [CrossRef]
22. Bowen, G.J.; Wassenaar, L.I.; Hobson, K.A. Global application of stable hydrogen and oxygen isotopes to wildlife forensics. *Oecologia* **2005**, *143*, 337–348. [CrossRef] [PubMed]
23. Terzer, S.; Wassenaar, L.I.; AraguásAraguás, L.J.; Aggarwal, P.K. Global isoscapes for δ18o and δ2h in precipitation: Improved prediction using regionalized climatic regression models. *Hydrol. Earth Syst. Sci.* **2013**, *17*, 4713–4728. [CrossRef]
24. Dutton, A.; Wilkinson, B.H.; Welker, J.M.; Bowen, G.J.; Lohmann, K.C. Spatial distribution and seasonal variation in 18o/16o of modern precipitation and river water across the conterminous USA. *Hydrol. Process.* **2010**, *19*, 4121–4146. [CrossRef]
25. Bowen, G.J. Water balance model for mean annual hydrogen and oxygen isotope distributions in surface waters of the contiguous USA. *J. Geophys. Res. Biogeosci.* **2015**, *116*, 105–112.
26. Cockerton, H.E.; Street-Perrott, F.A.; Leng, M.J.; Barker, P.A.; Horstwood, M.S.A.; Pashley, V. Stable-isotope (H, O, and Si) evidence for seasonal variations in hydrology and si cycling from modern waters in the Nile Basin: Implications for interpreting the quaternary record. *Quat. Sci. Rev.* **2013**, *66*, 4–21. [CrossRef]
27. Geldern, R.V.; Kuhlemann, J.; Schiebel, R.; Taubald, H.; Barth, J.A.C. Stable water isotope patterns in a climate change hotspot: The isotope hydrology framework of corsica (western mediterranean). *Isot. Environ. Health Stud.* **2014**, *50*, 184. [CrossRef]
28. Wen, R.; Tian, L.; Liu, F.; Qu, D. Lake water isotope variation linked with the in-lake water cycle of the alpine Bangong Co, arid western Tibetan Plateau. *Arct. Antarct. Alp. Res.* **2016**, *48*, 563–580. [CrossRef]
29. Calligaris, C.; Mezga, K.; Slejko, F.F.; Urbanc, J.; Zini, L. Groundwater characterization by means of conservative (d18O and d2H) and non-conservative (87Sr/86Sr) isotopic values: The Classical Karst Region aquifer case (Italy–Slovenia). *Geosciences* **2018**, *8*, 321. [CrossRef]
30. Yi, Y.; Gibson, J.J.; Cooper, L.W.; Hélie, J.F.; Birks, S.J.; McClelland, J.W.; Peterson, B.J. Isotopic signals (18O, 2H, 3H) of six major rivers draining the pan-arctic watershed. *Glob. Biogeochem. Cycles* **2012**, *26*. [CrossRef]
31. IAEA. Results of a coordinated research project 2002–2006. In *Monitoring Isotopes in Rivers: Creation of the Global Network of Isotopes in Rivers (GNIR)*; International Atomic Energy Agency: Vienna, Austria, 2012.
32. Penna, D.; Engel, M.; Bertoldi, G.; Comiti, F. Towards a tracer-based conceptualization of meltwater dynamics and streamflow response in a glacierized catchment. *Hydrol. Earth Syst. Sci.* **2017**, *21*, 23–41. [CrossRef]
33. Penna, D.; Engel, M.; Mao, L.; Dell'Agnese, A.; Bertoldi, G.; Comiti, F. Tracer-based analysis of spatial and temporal variations of water sources in a glacierized catchment. *Hydrol. Earth Syst. Sci.* **2014**, *18*, 5271–5288. [CrossRef]
34. Engel, M.; Penna, D.; Bertoldi, G.; Dell'Agnese, A.; Soulsby, C.; Comiti, F. Identifying run-off contributions during melt-induced run-off events in a glacierized alpine catchment: Identifying Run-off Contributions in a Glacierized Catchment. *Hydrol. Process.* **2016**, *30*, 343–364. [CrossRef]
35. Binet, S.; Joigneaux, E.; Pauwels, H.; Albéric, P.; Fléhoc, C.; Bruand, A. Water exchange, mixing and transient storage between a saturated karstic conduit and the surrounding aquifer: Groundwater flow modeling and inputs from stable water isotopes. *J. Hydrol.* **2017**, *544*, 278–289. [CrossRef]
36. Getdata-graph-digitizer.com. Digitize Graphs and Plots—GetData Graph Digitizer—Graph Digitizing Software. 2019. Available online: http://getdata-graph-digitizer.com/ (accessed on 23 January 2019).
37. Boschetti, T.; Cifuentes, J.; Iacumin, P.; Selmo, E. Local Meteoric Water Line of Northern Chile (18 S–30 S): An Application of Error-in-Variables Regression to the Oxygen and Hydrogen Stable Isotope Ratio of Precipitation. *Water* **2019**, *11*, 791. [CrossRef]

38. Crawford, J.; Hughes, C.E.; Lykoudis, S. Alternative least squares methods for determining the meteoric water line, demonstrated using GNIP data. *J. Hydrol.* **2014**, *519*, 2331–2340. [CrossRef]
39. Carr, J.R. Orthogonal regression: A teaching perspective. *Int. J. Math. Educ. Sci. Technol.* **2012**, *43*, 134–143. [CrossRef]
40. Fick, S.E.; Hijmans, R.J. Worldclim 2: New 1-km spatial resolution climate surfaces for global land areas. *Int. J. Climatol.* **2017**, *37*, 4302–4315. [CrossRef]
41. Zomer, R.J.; Bossio, D.A.; Trabucco, A.; Yuanjie, L.; Gupta, D.C.; Singh, V.P. IWMI Research Report 122. In *Trees and Water: Smallholder Agroforestry on Irrigated Lands in Northern India*; International Water Management Institute: Colombo, Sri Lanka, 2007; p. 45.
42. Zomer, R.J.; Trabucco, A.; Bossio, D.A.; van Straaten, O.; Verchot, L.V. Climate change mitigation: A spatial analysis of global land suitability for clean development mechanism afforestation and reforestation. *Agric. Ecosyst. Envir.* **2008**, *126*, 67–80. [CrossRef]
43. New, M.; Lister, D.; Hulme, M.; Makin, I. A high-resolution data set of surface climate over global land areas. *Clim. Res.* **2002**, *21*, 1–25. [CrossRef]
44. Lehner, B.; Grill, G. Global river hydrography and network routing: Baseline data and new approaches to study the world's large river systems. *Hydrol. Process.* **2013**, *27*, 2171–2186. Available online: www.hydrosheds.org (accessed on 30 January 2018). [CrossRef]
45. Wasserstein, R.L.; Lazar, N.A. The asa"s statement on p-values: Context, process, and purpose. *Am. Stat.* **2016**, *70*, 129–133. [CrossRef]
46. Britt, H. Model selection and Akaike's information criterion (AIC): The general theory and its analytical extensions. *Psychometrika* **1987**, *52*, 345–370.
47. Sugiura, N. Further analysis of the data by Akaike's information criterion of model fitting. *Suri-Kagaku Math. Sci.* **1978**, *153*, 12–18. [CrossRef]
48. Gooseff, M.N.; Lyons, W.B.; McKnight, D.M.; Vaughn, B.H.; Fountain, A.G.; Dowling, C. A stable isotopic investigation of a polar desert hydrologic system, McMurdo Dry Valleys, Antarctica. *Arct. Antarct. Alp. Res.* **2006**, *38*, 60–71. [CrossRef]
49. Yde, J.C.; Knudsen, N.T.; Steffensen, J.P.; Carrivick, J.L.; Hasholt, B.; Ingeman-Nielsen, T.; Roberts, D.H.; Oerter, H.; Mernild, S.H.; Russell, A.J.; et al. Stable oxygen isotope variability in two contrasting glacier river catchments in Greenland. *Hydrol. Earth Syst. Sci.* **2016**, *20*, 5841–5893. [CrossRef]
50. Craig, H. Isotopic variations in meteoric waters. *Science* **1961**, *133*, 1702–1703. [CrossRef]
51. Gourcy, L.L.; Groening, M.; Aggarwal, P.K. Stable oxygen and hydrogen isotopes in precipitation. In *Isotopes in the Water Cycle*; Springer: Berlin/Heidelberg, Germany, 2005; pp. 39–51.
52. Thomas, E.M.; Lin, H.; Duffy, C.J.; Sullivan, P.L.; Jin, L. Spatiotemporal patterns of water stable isotope compositions at the shale hills critical zone observatory: Linkages to subsurface hydrologic processes. *Vadose Zone J.* **2013**, *12*, 4949–4960. [CrossRef]
53. Allen, S.T.; Brooks, J.R.; Keim, R.F.; Bond, B.J.; Mcdonnell, J.J. The role of pre-event canopy storage in throughfall and stemflow by using isotopic tracers. *Ecohydrology* **2014**, *7*, 858–868. [CrossRef]
54. Morgenstern, U.; Stewart, M.K.; Stenger, R. Dating of streamwater using tritium in a post nuclear bomb pulse world: Continuous variation of mean transit time with streamflow. *Hydrol. Earth Syst. Sci.* **2010**, *14*, 2289–2301. [CrossRef]
55. Mcguire, K.J.; Mcdonnell, J.J. A review and evaluation of catchment transit time modeling. *J. Hydrol.* **2006**, *330*, 543–563. [CrossRef]
56. Moran, P.A. Notes on continuous stochastic phenomena. *Biometrika* **1950**, *37*, 17–23. [CrossRef] [PubMed]
57. Winnick, M.J.; Chamberlain, C.P.; Caves, J.K.; Welker, J.M. Quantifying the isotopic 'continental effect'. *Earth Planet. Sci. Lett.* **2014**, *406*, 123–133. [CrossRef]
58. Natural Earth. Rivers + Lake Centerlines. 2018. Available online: http://www.naturalearthdata.com/downloads/10m-physical-vectors/10m-rivers-lake-centerlines/ (accessed on 6 March 2018).
59. Aggarwal, P.K.; Gat, J.R.; Froehlich, K.F. *Isotopes in the Water Cycle: Past, Present and Future of a Developing Science*; Springer: Berlin/Heidelberg, Germany, 2005.
60. Cartwright, I.; Weaver, T.R.; Simmons, C.T.; Fifield, L.K.; Lawrence, C.R.; Chisari, R.; Varley, S. Physical hydrogeology and environmental isotopes to constrain the age, origins, and stability of a low-salinity groundwater lens formed by periodic river recharge: Murray Basin, Australia. *J. Hydrol.* **2010**, *380*, 203–221. [CrossRef]

61. Meier, S.D.; Atekwana, E.A.; Molwalefhe, L.; Atekwana, E.A. Processes that control water chemistry and stable isotopic composition during the refilling of Lake Ngami in semiarid northwest Botswana. *J. Hydrol.* **2015**, *527*, 420–432. [CrossRef]
62. Mekiso, F.A.; Ochieng, G.M. Stable water isotopes as tracers at the Middle Mohlapitsi catchment/Wetland, South Africa. *Int. J. Eng. Technol.* **2014**, *6*, 1728–1736.
63. Baer, T.; Barbour, S.L.; Gibson, J.J. The stable isotopes of site wide waters at an oil sands mine in Northern Alberta, Canada. *J. Hydrol.* **2016**, *541*, 1155–1164. [CrossRef]
64. Gibson, J.J.; Reid, R. Stable isotope fingerprint of open-water evaporation losses and effective drainage area fluctuations in a subarctic shield watershed. *J. Hydrol.* **2010**, *381*, 142–150. [CrossRef]
65. Poage, M.A.; Chamberlain, C.P. Empirical relationships between elevation and the stable isotope composition of precipitation and surface waters: Considerations for studies of paleoelevation change. *Am. J. Sci.* **2001**, *301*, 1–15. [CrossRef]